Research Article | Vol. 8, No. 3 | 1 Mar 2017 | BIOMEDICAL OPTICS EXPRESS 1712
Biomedical Optics EXPRESS

Label-free protein sensing by employing blue phase liquid crystal

MON-JUAN LEE,[1,4] CHUNG-HUAN CHANG,[2] AND WEI LEE[3,*]

[1]*Department of Bioscience Technology, Chang Jung Christian University, Guiren Dist., Tainan 71101, Taiwan*
[2]*Institute of Photonic System, College of Photonics, National Chiao Tung University, Guiren Dist., Tainan 71150, Taiwan*
[3]*Institute of Imaging and Biomedical Photonics, College of Photonics, National Chiao Tung University, Guiren Dist., Tainan 71150, Taiwan*
[4]*mjlee@mail.cjcu.edu.tw*
**wlee@nctu.edu.tw*

Abstract: Blue phases (BPs) are mesophases existing between the isotropic and chiral nematic phases of liquid crystals (LCs). In recent years, blue phase LCs (BPLCs) have been extensively studied in the field of LC science and display technology. However, the application of BPLCs in biosensing has not been explored. In this study, a BPLC-based biosensing technology was developed for the detection and quantitation of bovine serum albumin (BSA). The sensing platform was constructed by assembling an empty cell with two glass slides coated with homeotropic alignment layers and with immobilized BSA atop. The LC cells were heated to isotropic phase and then allowed to cool down to and maintained at distinct BP temperatures for spectral measurements and texture observations. At BSA concentrations below 10^{-6} g/ml, we observed that the Bragg reflection wavelength blue-shifted with increasing concentration of BSA, suggesting that the BP is a potentially sensitive medium in the detection and quantitation of biomolecules. By using the BPLC at 37 °C and the same polymorphic material in the smectic A phase at 20 °C, two linear correlations were established for logarithmic BSA concentrations ranging from 10^{-9} to 10^{-6} g/ml and from 10^{-6} to 10^{-3} g/ml. Our results demonstrate the potential of BPLCs in biosensing and quantitative analysis of biomolecules.

OCIS codes: (160.3710) Liquid crystals; (160.1585) Chiral media; (170.0170) Medical optics and biotechnology; (230.3720) Liquid-crystal devices.

References and Links

1. R. J. Carlton, J. T. Hunter, D. S. Miller, R. Abbasi, P. C. Mushenheim, L. N. Tan, and N. L. Abbott, "Chemical and biological sensing using liquid crystals," Liq. Cryst. Rev. **1**(1), 29–51 (2013).
2. Y. Y. Luk, M. L. Tingey, D. J. Hall, B. A. Israel, C. J. Murphy, P. J. Bertics, and N. L. Abbott, "Using liquid crystals to amplify protein-receptor interactions: Design of surfaces with nanometer-scale topography that present histidine-tagged protein receptors," Langmuir **19**(5), 1671–1680 (2003).
3. B. H. Clare and N. L. Abbott, "Orientations of nematic liquid crystals on surfaces presenting controlled densities of peptides: amplification of protein-peptide binding events," Langmuir **21**(14), 6451–6461 (2005).
4. S. Munir and S. Y. Park, "Liquid crystal-Based DNA biosensor for myricetin detection," Sens. Actuators B Chem. **233**, 559–565 (2016).
5. P. Popova, L. W. Honakerb, E. E. Kooijmanc, E. K. Manna, and A. I. Jáklib, "A liquid crystal biosensor for specific detection of antigens," Sens. Biosensing Res. **8**, 31–35 (2016).
6. M. Khan, A. R. Khan, J. H. Shin, and S. Y. Park, "A liquid-crystal-based DNA biosensor for pathogen detection," Sci. Rep. **6**, 22676 (2016).
7. N. A. Lockwood, J. C. Mohr, L. Ji, C. J. Murphy, S. P. Palecek, J. J. dePablo, and N. L. Abbott, "Thermotropic liquid crystals as substrates for imaging the reorganization of matrigel by human embryonic stem cells," Adv. Funct. Mater. **16**(5), 618–624 (2006).
8. H.-W. Su, Y.-H. Lee, M.-J. Lee, Y.-C. Hsu, and W. Lee, "Label-free immunodetection of the cancer biomarker CA125 using high-Δn liquid crystals," J. Biomed. Opt. **19**(7), 077006 (2014).
9. S. H. Sun, M. J. Lee, Y. H. Lee, W. Lee, X. Song, and C. Y. Chen, "Immunoassays for the cancer biomarker CA125 based on a large-birefringence nematic liquid-crystal mixture," Biomed. Opt. Express **6**(1), 245–256 (2014).

#281647 https://doi.org/10.1364/BOE.8.001712
Journal © 2017 Received 28 Nov 2016; revised 23 Jan 2017; accepted 14 Feb 2017; published 21 Feb 2017

Biomedical Optics EXPRESS

10. H. W. Su, M. J. Lee, and W. Lee, "Surface modification of alignment layer by ultraviolet irradiation to dramatically improve the detection limit of liquid-crystal-based immunoassay for the cancer biomarker CA125," J. Biomed. Opt. **20**(5), 57004 (2015).
11. H. G. Lee, S. Munir, and S. Y. Park, "Cholesteric Liquid Crystal Droplets for Biosensors," ACS Appl. Mater. Interfaces **8**(39), 26407–26417 (2016).
12. Y. C. Hsiao, Y. C. Sung, M. J. Lee, and W. Lee, "Highly sensitive color-indicating and quantitative biosensor based on cholesteric liquid crystal," Biomed. Opt. Express **6**(12), 5033–5038 (2015).
13. S. L. Helfinstine, O. D. Lavrentovich, and C. J. Woolverton, "Lyotropic liquid crystal as a real-time detector of microbial immune complexes," Lett. Appl. Microbiol. **43**(1), 27–32 (2006).
14. C. Y. Xue, S. A. Khan, and K. L. Yang, "Exploring optical properties of liquid crystals for developing label-free and high-throughput microfluidic immunoassays," Adv. Mater. **21**(2), 198–202 (2009).
15. V. J. Aliño, P. H. Sim, W. T. Choy, A. Fraser, and K. L. Yang, "Detecting proteins in microfluidic channels decorated with liquid crystal sensing dots," Langmuir **28**(50), 17571–17577 (2012).
16. T. Govindaraju, P. J. Bertics, R. T. Raines, and N. L. Abbott, "Using measurements of anchoring energies of liquid crystals on surfaces to quantify proteins captured by immobilized ligands," J. Am. Chem. Soc. **129**(36), 11223–11231 (2007).
17. C. H. Lin, M. J. Lee, and W. Lee, "Bovine serum albumin detection and quantitation based on capacitance measurements of liquid crystals," Appl. Phys. Lett. **109**(9), 093703 (2016).
18. H. Kikuchi, "Liquid crystalline blue phases," Struct. Bonding **128**, 99–117 (2008).
19. M. D. A. Rahman, S. Mohd Said, and S. Balamurugan, "Blue phase liquid crystal: strategies for phase stabilization and device development," Sci. Technol. Adv. Mater. **16**(3), 033501 (2015).
20. D. C. Wright and N. D. Mermin, "Crystalline liquids: The blue phases," Rev. Mod. Phys. **61**(2), 385–433 (1989).
21. H. Kikuchi, M. Yokota, Y. Hisakado, H. Yang, and T. Kajiyama, "Polymer-stabilized liquid crystal blue phases," Nat. Mater. **1**(1), 64–68 (2002).
22. E. Karatairi, B. Rozic, Z. Kutnjak, V. Tzitzios, G. Nounesis, G. Cordoyiannis, J. Thoen, C. Glorieux, and S. Kralj, "Nanoparticle-induced widening of the temperature range of liquid-crystalline blue phases," Phys. Rev. E Stat. Nonlin. Soft Matter Phys. **81**(4 Pt 1), 041703 (2010).
23. S. C. Chen, P. C. Wu, and W. Lee, "Dielectric and phase behaviors of blue-phase liquid crystals," Opt. Mater. Express **4**(11), 2392–2400 (2014).
24. Y. Moriyama, E. Watanabe, K. Kobayashi, H. Harano, E. Inui, and K. Takeda, "Secondary structural change of bovine serum albumin in thermal denaturation up to 130 ° C and protective effect of sodium dodecyl sulfate on the change," J. Phys. Chem. B **112**(51), 16585–16589 (2008).
25. V. A. Borzova, K. A. Markossian, N. A. Chebotareva, S. Y. Kleymenov, N. B. Poliansky, K. O. Muranov, V. A. Stein-Margolina, V. V. Shubin, D. I. Markov, and B. I. Kurganov, "Kinetics of thermal denaturation and aggregation of bovine serum albumin," PLoS One **11**(4), e0153495 (2016).
26. V. Sharma, A. Kumar, P. Ganguly, and A. M. Biradar, "Highly sensitive bovine serum albumin biosensor based on liquid crystal," Appl. Phys. Lett. **104**(4), 043705 (2014).
27. T. T. Nguyen, G. R. Han, C. H. Jang, and H. Ju, "Optical birefringence of liquid crystals for label-free optical biosensing diagnosis," Int. J. Nanomedicine **10**, 25–32 (2015).

1. Introduction

Biological detection by liquid crystals (LCs) is an emerging new field in biophotonics that is realized through biomolecules immobilized on solid surfaces or confined in LC–aqueous interfaces, or by utilizing LC-in-water droplets [1]. Traditional LC-based biosensing employs nematic LCs such as 5CB, which is the most extensively applied sensing medium in the detection of biomolecules such as proteins, peptides, and DNA, as well as biomolecular interactions such as the specific binding between antigen and antibody [2–5]. Besides 5CB, a wide variety of LC and LC mixtures are invented in the liquid-crystal display (LCD) industry, but their applications in biosensing are relatively scarce. A label-free DNA biosensor based on the nematic LC, E7, was designed for the detection of complementary single-stranded DNAs from pathogens [6]. Moreover, TL205, a nematic LC of low cytotoxicity, served as the substrate for the imaging of human embryonic stem cells [7]. By exploiting the large birefringence of another nematic LC, HDN, we demonstrated that the increased birefringence is critical to lowering the detection limit of CA125, a cancer biomarker, in a LC-based immunoassay [8–10]. For biological detection with other phases of LCs, cholesteric LCs (CLCs), produced by incorporating a chiral dopant in nematic LCs, were utilized as droplets in the design of glucose and cholesterol biosensors [11]. We also established a color-indicating protein biosensor facilitated by vertically aligned CLCs [12]. A real-time detector based on lyotropic chromonic liquid crystals, a different category of LCs as opposed to nematic ones, was developed to monitor microbial immunocomplexes [13].

Biomedical Optics EXPRESS

The basic principle underlying LC-based biosensing is that the optical texture of LCs changes with respect to the type and amount of biomolecules present on an LC aligning layer or at a LC–aqueous interface. However, to quantitate the amount of biomolecules, it is necessary to explore the correlation of biomolecular concentration to other measurable properties of LCs. Quantitative strategies were proposed for 5CB-based detection of biomolecules in microfluidic channels, in which the length of bright area or the number of bright LC dots were proportional to the concentration of antibodies or bovine serum albumin (BSA), a common protein standard [14, 15]. In addition, the anchoring energy of LCs is measured in an attempt to quantitate the concentration of antibodies specifically bound to peptide ligands [16]. By exploiting the Bragg reflection of CLC and transmission spectroscopy, the concentration of BSA can be correlated with the minimum transmittance or bandwidth of incident light [12]. Through the measurement of capacitance properties of LCs under an externally applied electric field, we observed that BSA quantitation can also be achieved by measuring the voltage-dependent capacitance of nematic LC cells containing immobilized BSA [17]. Nevertheless, quantitative biosensing technology based on LCs remains at an early stage of development.

In this work, we attempt to explore the potential of blue phase liquid crystals (BPLCs) in LC-based biosensing. BPLCs are unique phases that exist in a defined temperature range within the isotropic–chiral-nematic phase transition [18–20]. They are self-assembled and topologically ordered liquid crystalline materials with a reduction of symmetry, consisting of cubic lattices of double-twisted cylinders of liquid crystal (LC) molecules. Depending on the chirality and the packing of double-twisted cylinders giving a specific cubic array of defects, the blue phases (BPs) can be categorized into BPI, BPII and BPIII, with BPIII resembling the isotropic phase, and BPII and BPI appearing successively during phase transitions in the cooling process. One of the distinctive properties of a BPLC, like the chiral nematic (*viz.* CLC) phase characterized by a helical, twisted structure, is Bragg's reflection in the visible spectrum, giving rise to a reflected color. Due to their fast field-response governed by the Kerr effect, BPs are considered promising for future applications in the development of LC display and other photonic technologies. Current studies of BPLCs focus mainly on the stabilization of BP, which generally exists within a relatively narrow temperature range. Strategies such as addition of polymer or nanoparticles have been reported to widen the BP temperature range [21, 22].

On the basis of our previous studies, here we aim to develop a quantitative biosensing platform with a BPLC as the sensing element by establishing a protein assay with BSA. Protein assay is a fundamental procedure for protein quantitation in the laboratory. It is applied not only to purified proteins, but also to cell lysates or crude extracts from bacteria, animal or plant cells that contain mixtures of proteins. Although proteins can be directly detected with ultraviolet absorption spectroscopy, more commonly used protein assays such as the Bradford or Lowry assays are colorimetric, which rely on dye binding or metal chelation of proteins to achieve higher sensitivity. The absorbance of the resulting protein complex at a specific wavelength within the visible spectrum is used to calculate the protein concentration according to Beer's law. In such quantitative analysis, BSA is often selected as the protein standard to create a calibration curve of absorbance vs. BSA concentration. The concentration of protein samples, irrespective of their protein contents and molecular weights compared to BSA, is then interpolated from the calibration curve using their measured absorbances. Traditional protein assays are easy to perform with an absorption spectrometer, but the concentration range of linearity is usually limited to an order of magnitude. In LC-based protein assays, linearity may be expanded to three to four orders of magnitude according to our previous reports [12, 17]. By controlling the temperature within the ranges of the BP and smectic A (SmA) phase existence, we analyzed the transmission spectra of BPLC interfaced with BSA at various concentrations along with complementary optical texture

Biomedical Optics EXPRESS

observations. Results from this study are expected to provide insights into the biosensing capabilities of BPLCs and a novel alternative to protein assays.

2. Experiment

The LC used in this study was prepared by mixing the eutectic nematic host E7 (n_e = 1.7472, n_o = 1.5217) with the chiral dopant S811 at 30.1 wt% [23]. A LC cell, with a thin layer of the mixture sandwiched between two glass slides, was prepared as described in our previous study [12]. Glass slides were washed successively with detergent and deionized water accompanied by ultrasonication at room temperature. The clean glass slides were coated with the surfactant dimethyloctadecyl[3-(trimethoxysilyl)propyl] ammonium chloride (DMOAP, Sigma–Aldrich) for the homeotropic alignment of LC, followed by immobilization with various concentrations of BSA (Sigma–Aldrich) on the DMOAP layers. Each empty cell was fabricated by aligning two thus-coated glass slides separated by ball spacers of ~8 μm in diameter, with BSA-covered surfaces facing each other. The empty cell was then filled with the LC by capillary action. The optical texture of each LC cell was determined by an Olympus BX51 polarized optical microscope, while the transmission spectra were taken with an Ocean Optics HR2000 + high-resolution USB fiber-optic spectrometer (0.2-nm resolution) equipped with an ILX511b detector (Fig. 1). To obtain the BP structure, the concoction confined in a cell was heated to isotropic phase (40 °C) and then cooled at a constant rate of 0.1 °C/min, during which the LC texture and transmission spectra were recorded over time. Temperature control was accomplished by a Linkam T95-PE system with a temperature stability and accuracy of ± 0.1 °C and a Wise Life TEC controller CDSI5008RRA with an accuracy of ± 0.5 °C in conjunction with the microscope and the spectrometer, respectively.

3. Results and discussion

The commonly available chiral dopant S811, in combination with the LC host E7, was chosen in this study to produce a chiral LC with BP appearing in the temperature range around 32–38 °C, which is within the physiological temperature regime of most mammalian cells to ensure that the activity of biomolecules remains unaffected. Although BPs exist in a narrow temperature range, the composition of BPLCs used in this study is relatively more thermally stable than traditional BPLCs with smaller temperature range (0.5–1 °C) of BP existence [19].

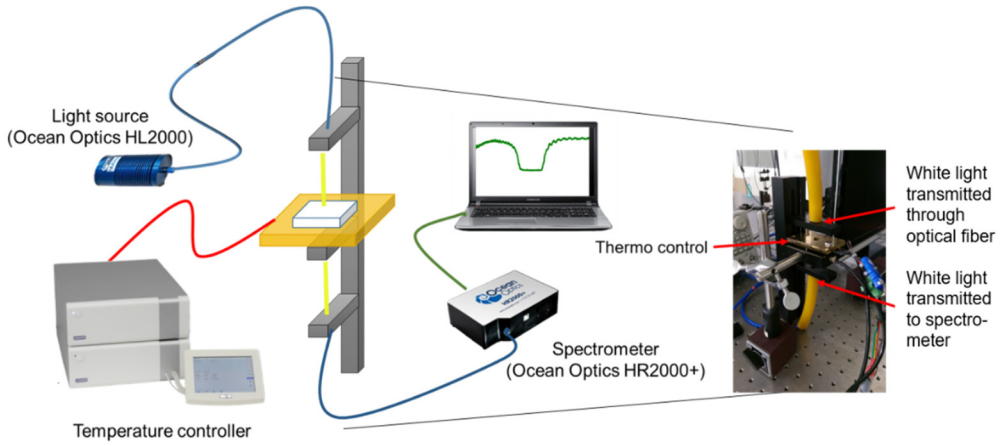

Fig. 1. System diagram of transmission spectroscopic measurement for the BPLC-based protein assay.

The resulting LC cells have cell gaps of 7.6 ± 0.5 μm. When the LC was heated to isotropic phase and allowed to cool down, the optical texture shifted to the BP at 38.1 °C, to the cholesteric phase at 31.7 °C, to the twist grain boundary (TGBA) phase at 28.1 °C, and

Biomedical Optics EXPRESS

finally to the SmA phase at 27.4 °C as shown in Fig. 2. Studies on the thermostability of BSA suggest that BSA is denatured and aggregated at temperatures above 60 °C, and the structure of BSA is partially damaged when heated to 50 °C [24, 25]. Therefore, the heating and cooling process for the phase transition of LCs should impose minimal effect on the structure and function of BSA as long as the temperature does not exceed 50 °C.

Under the induction of homeotropic alignment by DMOAP, the optical texture in BP changed with decreasing temperature, from a uniform color at 38 °C to that with scattered domains of bright spots at 35 °C (Fig. 3(a)). By monitoring the transmission spectra of the LC in BP, we found that the Bragg reflection blue-shifted from 670 to 530 nm with decreasing temperature (Fig. 3(b)). The decrease in wavelength with falling temperature followed a biphasic manner, with the wavelength reducing at a relatively lower rate from 39 to ~37 °C in comparison with that from ~36.5 to 33 °C (Fig. 3(c)). The BPII–BPI phase transition temperature, 36.8 ± 0.5 °C, can thus be deduced from the boundary of the two mesophases in the reflection-wavelength-versus-temperature plot.

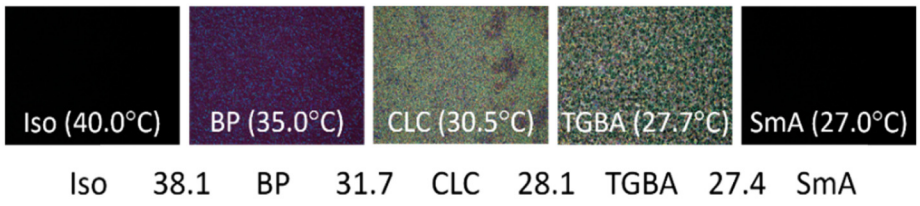

Fig. 2. Phase sequence and optical textures of E7 doped with 30.1-wt% S811 at various phases observed at decreasing temperatures.

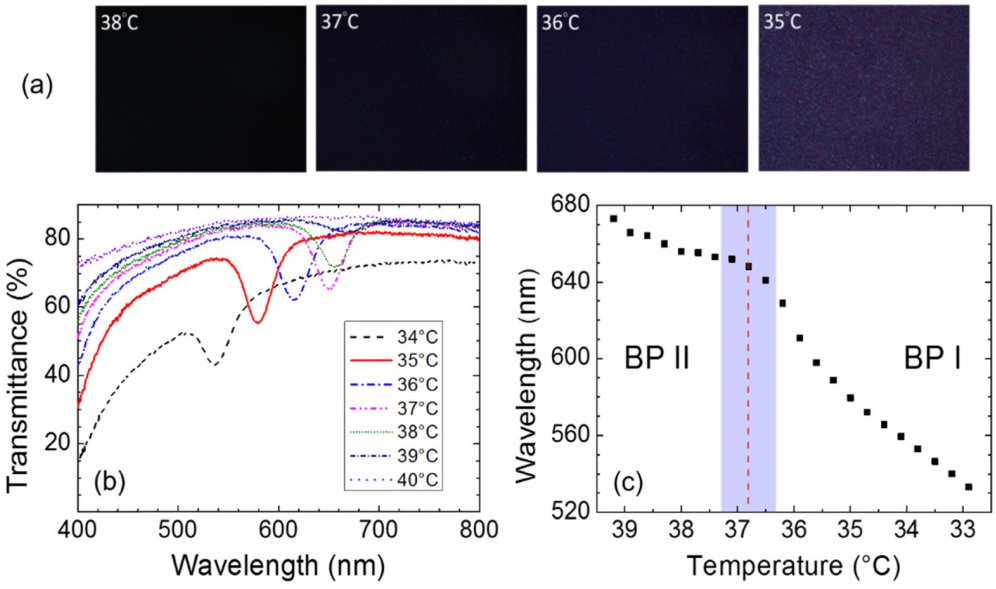

Fig. 3. Effect of temperature on the optical texture and transmission spectrum of BPLC. (a) The change in optical texture of a BPLC with temperature. (b) The transmission spectra of a BPLC at various temperatures. (c) The reflection wavelength plotted against the temperature, giving two regions corresponding to two different BP structures.

Biomedical Optics EXPRESS

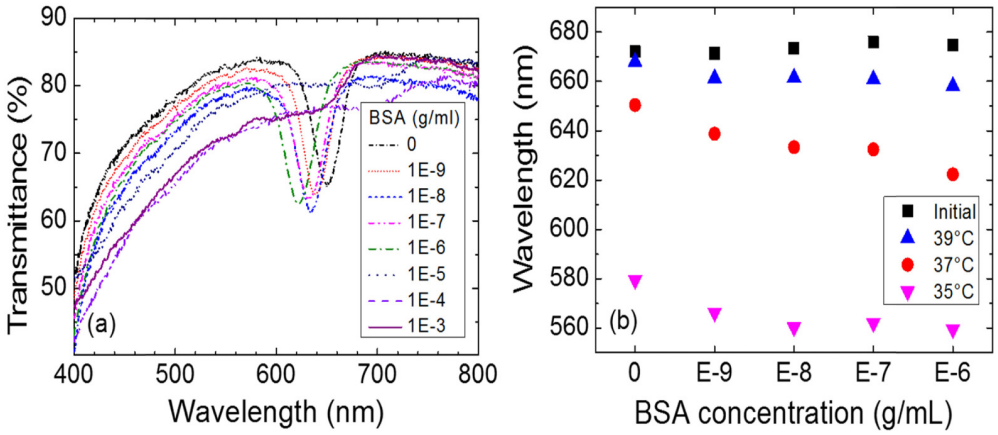

Fig. 4. Effect of BSA on the transmission spectrum of BPLC. (a) Transmission spectra of BPLCs in the presence of various concentrations of immobilized BSA at 37°C. (b) Correlation between reflection-peak wavelength and BSA concentration at three selected temperatures. The initial values were defined as the wavelengths in the first appearance of BP during the cooling process.

When BSA was immobilized on DMOAP, the homeotropic alignment of LC and the orientation of the BP lattice were disrupted, resulting in lattice disorder and blueshift of the reflection wavelength. As shown in Fig. 4(a), in the presence of 10^{-9}–10^{-6} g/ml BSA at 37 °C, the reflection wavelength of the BPLC decreased with increasing BSA concentration, while an explicit correlation of BSA concentration to peak reflection was not observed. Although BPLCs are intrinsically temperature-sensitive, giving rise to a significant change in transmission spectra with temperature (Fig. 3(a)), by employing a temperature controller with an accuracy of ± 0.5 °C or smaller, constant temperature can be maintained within a reasonable tolerance during transmission spectroscopic measurement, thus minimizing the variation in the Bragg reflection peak value at each temperature. We can therefore assume that the wavelength shift with BSA concentration observed at 37 °C (Fig. 4(a)) is due predominantly to change in the amount of BSA, instead of temperature oscillation. On the other hand, the transmission spectrometer used in this study has a resolution of 0.2 nm (FWHM), which is much smaller than the blueshift of the Bragg reflection peak in the transmission spectra within an order of magnitude change in BSA concentration (Fig. 4(a)). The level of blueshift from 10^{-9} to 10^{-6} g/ml BSA, though occurred within a narrow range of wavelength, is thus considered significantly correlated with the concentration of BSA.

At 35 and 39 °C, the decrease in Bragg's reflection wavelength with respect to BSA concentration was less significant compared with that at 37 °C, indicating that there exists an optimal temperature for the quantitation of biomolecules using the BP-based biosensing method (Fig. 4(b)). In addition, we found that the logarithmic BSA concentration was linearly correlated to the wavelength difference between the reflection wavelength at 37 °C (Fig. 4(a)) and the initial wavelength in the first appearance of BP during the cooling process in the presence of various BSA concentrations (see Fig. 5). A linear regression fit produced from such plot may facilitate protein quantitation using BSA as the standard protein.

Biomedical Optics EXPRESS

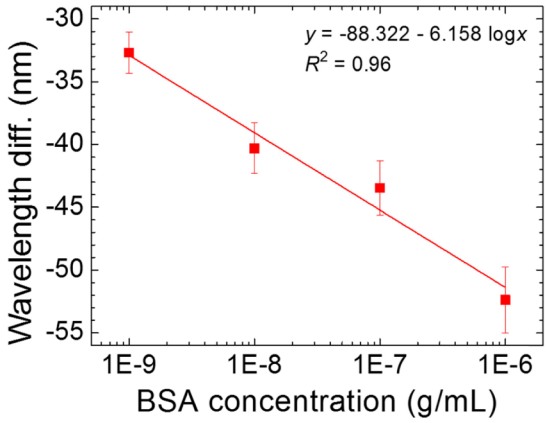

Fig. 5. Correlation of wavelength difference to BSA concentration at 37°C.

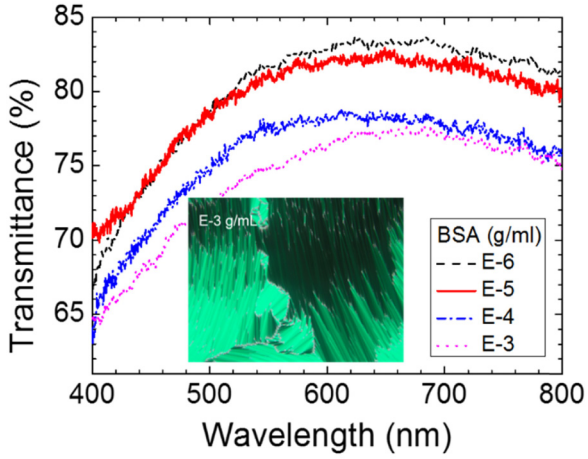

Fig. 6. Transmission spectra of the E7/S811 mixture in SmA phase in the presence of immobilized BSA of various concentrations at 20°C. Inset: optical texture of SmA in the presence of 10^{-3}-g/ml BSA at 20°C.

At BSA concentrations higher than 10^{-6} g/ml, no obvious BP reflection peak was observed in the transmission spectra (Fig. 4) due to the severe scattering caused by multi-domain boundaries, implying that the amount of BSA has reached a threshold at which the BP lattice cannot be properly formed. We therefore cooled the LC cell gradually to 20 °C to the SmA phase for the detection of BSA in the higher concentration range (10^{-6}–10^{-3} g/ml). As shown in Fig. 6 (see the inset), the optical texture of a LC in the presence of 10^{-3} g/ml BSA indicates that the SmA phase was formed at 20 °C. The amount of BSA cannot be easily identified through optical texture alone, because the optical texture was mostly in the dark state at BSA concentrations lower than 10^{-3} g/ml. We therefore exploited the transmission spectra of SmA phase at various BSA concentrations above 10^{-6} g/ml to assist in BSA quantitation (Fig. 6). It was observed that the overall transmittance decreased with increasing concentration of BSA, suggesting that the level of light scattering contributed by BSA molecules was related to the amount of BSA. By plotting the transmittance at 570 nm or the transmittance integral between 550 and 700 nm (where the maximal intensity of emission of the light source takes place) against the BSA concentration in logarithm, a linear correlation was found as shown in Fig. 7. Although the data are somewhat scattered, the coefficient of determination r^2 for the linear fit is still greater than 0.92 in each case.

Biomedical Optics EXPRESS

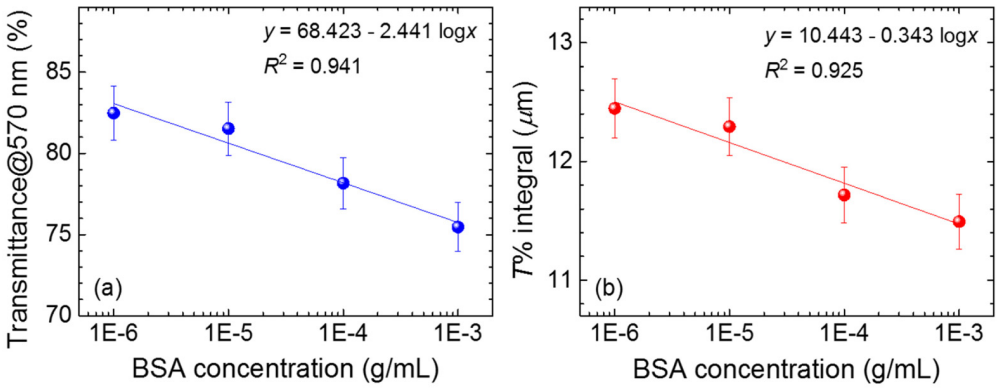

Fig. 7. Correlations of (a) the transmittance at 570 nm and (b) the transmittance integral between 550 and 700 nm to the BSA concentration in logarithm. The error bar is dominated by light scattering.

When BSA was immobilized on a DMOAP-coated glass surface, we observed that the detection limit of BPLC-based protein assay, 10^{-9} g/ml (15 pM) BSA, was similar to that based on voltage-dependent capacitance measurement of HDN, but was three orders of magnitude higher than that of the CLC-based protein assay (10^{-12} g/ml), as described in our previous work [12, 17]. Other studies on LC-based BSA detection demonstrated that biosensing with 5CB on a glass surface functionalized with gold nanoparticles resulted in a detection limit of 0.5 μg/ml (7.5 nM) BSA based on optical texture observation [26]. By immobilizing BSA on an Au-coated surface, a detection limit of 2.1 μM was achieved with 5CB as the sensing mesogen [27]. These comparisons indicate that the performance of LC-based biosensing depends not only on the type of mesogen used, but also on the surface modification, as well as the qualitative or quantitative analysis in conjunction with the technology.

For current protein assays such as the Bradford assay, the detection limit in a 96-well microplate format is 1.25 μg/ml BSA according to the protocols of commercial assay kits such as Bio-Rad Quick Start Bradford Protein Assay. Protein quantitation by UV detection is less accurate because the level of UV absorption varies with the amount of aromatic amino acids in each protein. The detection limit at 280 nm is 0.1–100 mg/ml BSA for Thermo Scientific NanoDrop spectrophotometers. Fluorescence detection offers a lower detection limit of 10 ng/ml BSA when a commercial assay kit such as Thermo Scientific NanoOrange® Protein Quantification Assay is used. With a detection limit (10^{-9} g/ml) comparable to fluorescence quantitation, BPLC-based protein assay may potentially be advantageous in the detection of low protein concentrations or diluted protein samples.

The fact that BSA can be quantitated by the BPLC sensing platform suggests that other proteins or protein mixtures can also bind nonspecifically to DMOAP and be quantitated in a similar fashion. Our results indicate that BPLCs were sensitive in the detection and quantitation of low concentrations of biomolecules, while at higher concentrations, the SmA phase provided a more suitable quantitative sensing platform. Consequently, to perform protein assay with the BPLC used in this work, it is necessary to ensure that the protein concentration is within the range of 10^{-9}–10^{-3} g/ml BSA (with molecular weight of 66,463 Da), which corresponds to 15 pM–15 μM of total protein. This can be achieved by diluting the protein sample at a known dilution ratio to concentrations within the limit of linearity (Fig. 5), a common practice in conventional protein assays.

Protein assays are less clinically related, but are fundamental in the determination of protein expression, in which the amount of a specific protein must be normalized to that of total protein in a biological sample. To extend current technique to clinical application, BSA

Biomedical Optics EXPRESS

can be substituted for an antibody specific for a disease-related biomarker, which is then reacted with a serum sample containing the biomarker to assess the detection specificity of BPLCs, as described in our previous work on the LC-based detection of the cancer biomarker CA125 [8–10]. Although the process of achieving and maintaining BPs may require further simplification to enhance practical application, results from this study provide the first implications that quantitative biosensors based on BPLCs may be realized with the fast development of BP-related photonic technologies.

4. Conclusions

A BPLC-based biosensing technology involving transmission spectroscopy has been demonstrated in this study for the quantitative analysis of BSA. The BP lattice was disturbed in the presence of BSA immobilized on the DMOAP layers for homeotropic anchoring of LC molecules, resulting in blueshift of the wavelength of the Bragg reflection. We found that the wavelength difference of the BPLC at 37 °C was linearly correlated to the BSA concentration in logarithm between 10^{-9} and 10^{-6} g/ml, and that the transmittance of the same LC in the SmA phase at 20 °C was linearly proportional to the logarithmic concentration in the range of 10^{-6} and 10^{-3} g/ml, rendering a total range of concentration-dependent correlation considerably wider than conventional protein assays. Accuracy or linearity within a narrow concentration range, which is characteristic of traditional protein assays, may not be achieved at the current stage of development, but is possible with further fine-tuning of the detection strategy to widen the range of blueshift in correlation with BSA concentration. To the best of our knowledge, this is the first demonstration of utilization of two distinct mesophases (BP and SmA) of a single LC material for biosensing. The principles of BPLC-based protein assay reported in this study can be extended to the detection of protein–protein interactions, such as the antigen–antibody immunoassay for clinical application. It is therefore concluded that BPLC is a promising sensing material for the development of LC-based biosensing technologies and of other biophotonics applications.

Funding

This work was financially supported by the Ministry of Science and Technology, Taiwan, under grant Nos. 104-2112-M-009-008-MY3 and 103-2633-B-309-001. W. Lee is the corresponding author and M.-J. Lee is the co-corresponding author.